Zhang et al. *NPG Asia Materials* (2023) 15:45
https://doi.org/10.1038/s41427-023-00492-x

NPG Asia Materials

ARTICLE Open Access

Magnetoactive microlattice metamaterials with highly tunable stiffness and fast response rate

Wenqiang Zhang[1], Jingzhuo Zhou[1], Yanwen Jia[1], Juzheng Chen[1], Yiru Pu[1], Rong Fan[1,2], Fanling Meng[3], Qi Ge[4] and Yang Lu[1,2,5]

Abstract

Active metamaterials with shapes or mechanical properties that can be controlled remotely are promising candidates for soft robots, flexible electronics, and medical applications. However, current active metamaterials often have long response times and short ranges of linear working strains. Here, we demonstrate magnetoactive microlattice metamaterials constructed from 3D-printed, ultra-flexible polymer shells filled with magnetorheological (MR) fluid. Under compressive stress, the magnetorheological fluid develops hydrostatic pressure, allowing for a linear compression strain of more than 30% without buckling. We further show that under a relatively low magnetic field strength (approximately 60 mT), the microlattices can become approximately 200% stiffer than those in a relaxed state, and the energy absorption increases ~16 times. Furthermore, our microlattices showed an ultra-low response time with "field on" and "field off" times of ~200 ms and ~50 ms, respectively. The ability to continuously tune the mechanical properties of these materials in real time make it possible to modulate stress–strain behavior on demand. Our study provides a new route toward large-scale, highly tunable, and remotely controllable metamaterials with potential applications in wearable exoskeletons, tactile sensors, and medical supports.

Introduction

Active mechanical metamaterials or field-responsive mechanical materials refer to materials with a complicated structure whose shapes and/or properties can be modulated by external stimulations such as heat[1–6], magnetic fields[7,8], and solvents[9–12]. The nature of these external stimulations gives makes it possible to remotely control these active materials, and they hold promise for applications in flexible electronics, soft robots[13], microelectromechanical systems (MEMS), and biomedical devices due to their minimally invasive nature[14,15]. Despite these advantages, most active mechanical metamaterials are limited by relatively long response times and thus poor controllability because the material responds by undergoing phase transitions or chemical reactions. For example, the response times of some 3D-printed thermally active structures are tens of minutes and even hours[14]. Some materials[16,17] are reported to have a short electrical response time, although an ultra-high voltage (~6 kV) is required to trigger millimeter-scale electroactive materials.

Magnetoactive or magnetic responsive materials are promising candidates for fast response times. Traditionally, they are composed of so-called ferromagnetic soft materials in which magnetized or magnetizable microparticles are uniformly dispersed in soft polymeric matrices. These particles apply micro-torques when applied magnetic fields drive the deformation of the structure. Current substrate materials are soft enough for magnetic fields to trigger large deformations, and various soft robots have been proposed[8,13,18,19].

To construct a loading bearing form, active materials are usually fabricated as lattices[20–24], and these structures are also referred to as metamaterials with advantages of light

Correspondence: Yang Lu (ylu1@hku.hk)
[1]Department of Mechanical Engineering, City University of Hong Kong, Kowloon, Hong Kong SAR, China
[2]Nano-Manufacturing Laboratory (NML), City University of Hong Kong Shenzhen Research Institute, Shenzhen, China
Full list of author information is available at the end of the article

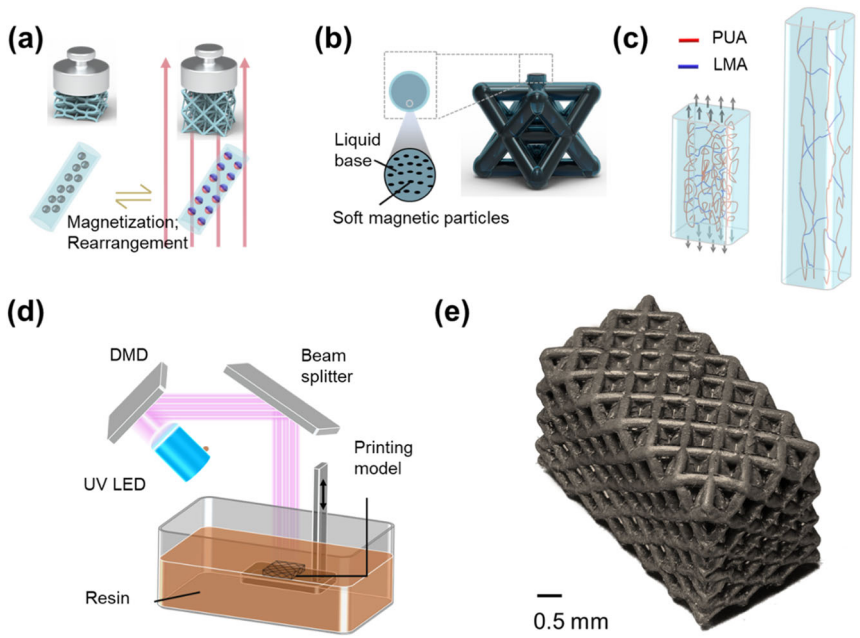

Fig. 1 The magnetoactive microlattice metamaterial composed of a 3D printed hollow polymer microlattice scaffold filled with MR fluid. **a** Illustration showing the tunability and reversibility of the MR fluid-filled microlattice to obtain enhanced strength in the presence of a magnetic field. **b** The configuration of our MR fluid-filled microlattice. **c** Schematic of the very stretchable polymer mainly composed of PUA and LMA. **d** Schematic of the Projection Microstereolithography technology. **e** MR fluid-filled truss with 6 by 3 by 4 octet units.

weight, tunable and adaptive building blocks (Fig. 1a), showing potential for applications in wearable exoskeletons, safety devices, and intravascular stents. Due to the presence of solid magnetic particles, the magnetoactive lattice usually is fabricated by the mold-assisting method, namely, the magnetoactive elastomers are cured within a hollow 3D printed mold, and then the mold is removed[23,24]. There are also studies of magnetorheological fluid-incorporated in lattices or foams[22,25]. Magnetorheological fluids are comprised of micro-scale soft magnetic particles uniformly suspended in a base fluid, and other additives are incorporated to prevent the particles from aggregating. The magnetorheological fluids have a larger volume fractions of magnetic particles (≥50%), and the magnetorheological fluids incorporated in metamaterials have wider ranges of available mechanical properties and faster response times than magnetic particles in soft matrices.

Despite the purported advantage, these magnetoactive lattices have two main drawbacks. First, a strong magnetic field (≥0.1 T) is required to induce an expected change in shape or mechanical response. An ultra-powerful Nd-Fe-B permanent magnetic alloy or Helmholtz coil working at high voltage is needed, but such apparatuses make the operation dangerous; the other challenge is the short linear strain and buckling of the base materials. Typically, the yield strains of most lattice materials are less than 10%, which makes the working range short[26–28]. Moreover, although magnetic substances present an almost linear relationship with the intensity of the magnetic field, the low modulus of soft materials leads to buckling at a very early stage. By harnessing the buckling, soft materials can generate sophisticated movement in soft robots[13]. However, buckling in lattice metamaterials lead to abrupt changes in mechanical properties, limiting the operating ranges of metamaterials[24,25].

Here, we adopt an ultra-flexible polymer shell that maximizes the tunable properties of an MR fluid, creating a liquid–solid dual-phase microlattice metamaterial (Fig. 1b) with a wide range (200%) of tunable stiffness. This microlattice exhibits continuously adjustable, programmable, predictive, rapid and reversible responses by facile application of a relatively weak magnetic field (60 mT).

Materials and methods

Here, we take advantage of a 3D-printable flexible polymer and magnetorheological (MR) fluid to create a flexible mechanical metamaterial. To obtain a wide range of tunable mechanical properties, the initial stiffness of the polymer substrate should be low. Therefore, this study uses a highly flexible polymer from BMF Boston Micro Fabrication (Shenzhen City, Guangdong Province, China), which is mainly composed of polyurethane acrylate (PUA), lauryl methacrylate (LMA), acryloylmorpholine (ACMO), and tetrahydrogen folic acid (THFA).

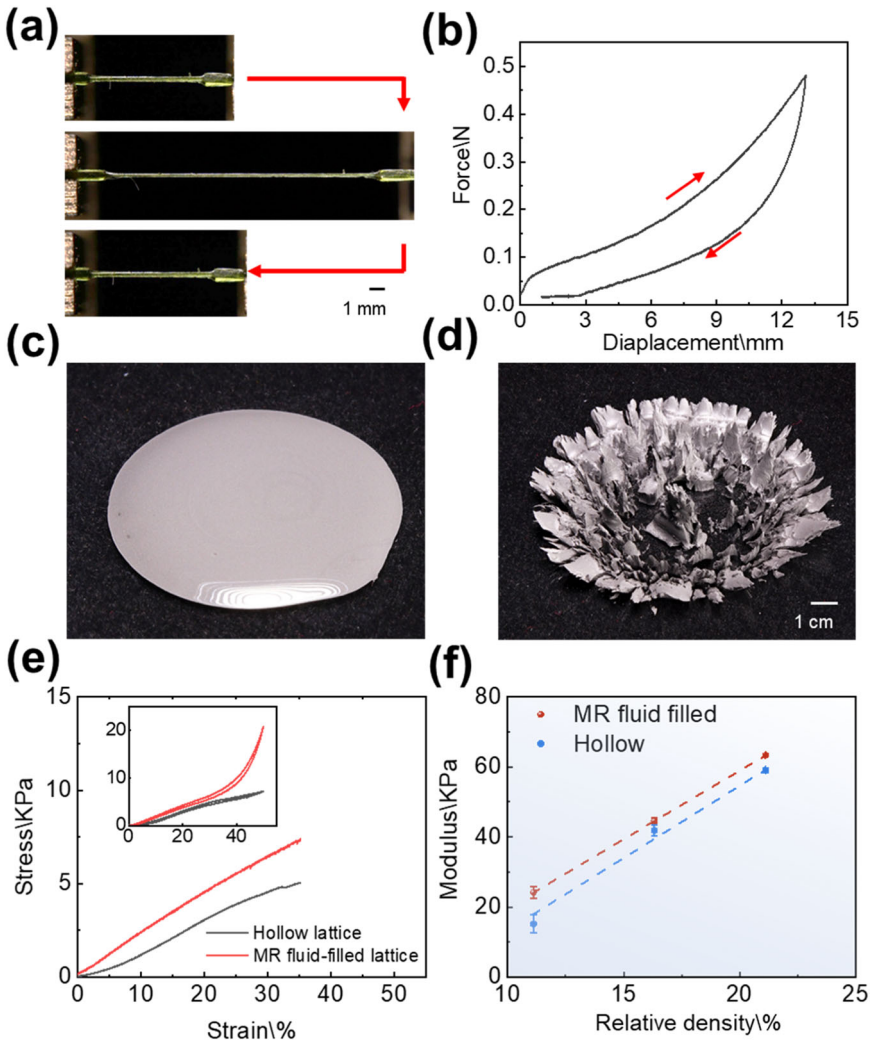

Fig. 2 Properties of the flexible and recoverable MR fluid-filled structure and microlattice. a Optical images of the PμSL-printed elastomer from 0 to 150% strain and then to ~20% strain. **b** Cyclic test curves of the printed elastomer. Shape response of the MR fluid under the application and withdrawal of a magnetic field. **c** The MR fluid spread on a planar substrate with a smooth surface in the absence of a magnetic field. **d** The MR fluid forming columns with the application of a magnetic field. **e** Compression curves of the MR fluid-filled octet microlattice and hollow microlattice. **f** Comparison of the stiffnesses of the hollow microlattice and MR fluid-filled microlattice.

Projection micro-stereolithographyy (PμSL) is employed to print the polymer to make 3D scaffolds (Fig. 1c). PμSL is a layer-by-layer printing technology with that provides high printing resolution without sacrificing printing area (Fig. 1d)[29]. Moreover, PμSL is a facile technology that can be used to fabricate airtight hollow scaffolds to construct liquid–solid dual-phase microlattice metamaterials[30].

First, a hollow octet lattice with an inlet is printed by PμSL. The inlet is immersed in MR fluid (BOHAI MATERIALS, A181). The sealed hollow lattice along with the MR fluid are placed under a vacuum. Then, the chamber is restored to atmospheric pressure, and the atmospheric pressure pushes the MR fluid into the hollow lattice. The result of a lattice filled with MR. The final step is sealing the inlet. The inlet is covered by liquid resin and solidified in a UV curing box.

Previous studies have proven the successful application of MR fluids in adaptive metamaterials in the forms of an open-cell foam and a cuboctahedron (bending-dominated lattice)[22,25]. In this study, we adopt a typical stretching-dominated lattice – octet (Fig. 1b). According to Maxwell's criterion, each joint connects more struts in a stretching-dominated lattice. In the octet lattice, the number of joint connections is up to twelve struts, 50% more than that of a cuboctahedron lattice. The traditional injection method remains challenging for a hollow octet lattice. Vacuum filling is an effective method to fill complex microchannels in 2D and 3D structures with MRs[30,31] with the advantages

of filling rates and a universal method for different topographies. Moreover, the vacuum filling process requires only a single inlet without considering the distribution of the outlet and inlet. Figure 1e demonstrates the viability of creating a larger number of MR fluid-filled (6 by 3 by 4) units (up to 72 units). This study also proves that it is possible to scale up our method for manufacturing compared with the traditional injection method with no more than 8 units[23,25].

Results and discussion

Mechanical properties

The experiment shows that this ultra-flexible polymer has a fracture strain of more than 200% (Fig. S1), which provides strong protection for our microlattice materials. Furthermore, the printed elastomer can be stretched to more than 150% of its initial length and almost recovers (Fig. 2a, b and Video S1). The mechanical properties of the MR fluid can be altered by introducing and withdrawing the magnetic field. When the magnetic field is removed, the fluid behaves a medium with unrestricted flow, and it can be regarded as an ultra-flexible material (Fig. 2c). Once a magnetic field is applied, the magnetic particles rearrange along the magnetic field direction (Fig. 2d). Thus, ultra-flexible and ultra-recoverable metamaterials can be obtained by combining these two materials. To visually demonstrate the flexibility and recoverability, a MR fluid-filled octet microlattice is severely compressed to densification by using a finger to apply pressure, and it recovers to the original state once the force is removed (Video S2).

For the convenience of mechanical testing, a 2 by 2 by 2 MR fluid-filled microlattice is chosen for most tests, and it is accepted that two cells in each direction are required to evaluate the observed behavior[15,32]. The mechanical properties of a hollow elastomer microlattice and an MR fluid-filled microlattice with a relative density of 11.1% (refers to the density of the polymer shell) are shown in Fig. 2e. The effective stiffness of the hollow microlattice is measured as 0.18 MPa. When filled with MR fluid, a slight increase in stiffness is observed compared with the hollow flexible polymer microlattice. The stress–strain curves are linear (Fig. 2e) with a linear strain of over 30%. Loading and unloading curves are shown in the inset picture to demonstrate the excellent recoverability of the flexible lattice. An in situ video (Video S3) indicates that the deformation is the rotation of the node. The presence of the MR fluid prevents the hollow lattice from buckling. Buckling is a common deformation mechanism in lattice materials but results in uncontrollable deformation[24,33,34]. Due to the hollow structure, the node rotates first, making the deformation localized at the node, leading the lattice struts to be essentially unloaded; the lattice buckles at low stress[35]. During the compression process, the MR fluid can develop hydrostatic stress in the closed lattice (Fig. 2f). Prolonged linear strain increases the working range of the MR-filled lattice.

The mechanical properties of PμSL-printed polymers depend on their characteristic sizes. For example, in the range of 20–60 μm, the fracture elongation and strength increase with decreasing size[5]. The normalized yield strength increases as the shell thickness decreases from 200 μm to 177 nm and 333 nm[36]. However, other researchers reported that the yield stress did not provide an insignificant dependent relationship for characteristic sizes in the range of 100–500 μm[30]. In this study, the different relative densities of the hollow lattice correspond to thicknesses of 100 μm and 150 μm and 200 μm. Therefore, in this study, we make a simplification that the yield stress and modulus of the polymer shell remain consistent.

Tunable stiffness and energy absorption ability

In addition to the deformation response induced by the magnetic field, the mechanical response is an attractive advantage of the MR fluid-filled microlattice. The interaction between the polarized particles increases with increasing magnetic field strength, which enables different stiffnesses under a magnetic field[25,37]. To characterize the mechanical performance of our MR fluid-filled microlattice, compression tests are conducted in a custom apparatus with aluminum platens, and the magnetic field is established by an electromagnet that can be controlled by a DC power adapter (Fig. 3a). The measured stiffness response as a function of magnetic field strength is shown (Fig. 3b, Table S1). With the presence of a magnetic field, the stiffness gradually increases, and the stiffness increases by approximately 200% at a magnetic field strength of 60 mT. Compared with previously studied metamaterials composed of MR fluid, the increment in stiffness of greater (4.03 MPa/T), while that of the previous study was 0.42 MPa/T[22]. The greater rate increasing stiffness is attributed to our ultra-flexible polymer shell and the relatively higher relative density of the MR fluid. However, structural topologies have a significant role here in the mechanical behavior of microlattice structures. Previous experiments and theories proved that the stretching-dominated lattice was more mechanically efficient with a higher stiffness-to-weight ratio (defined as E/ρ) than the bend-dominated counterpart[38].

The stiffness of the MR fluid-polymer is determined[15]:

$$E_{MR} = \frac{\sigma_{eff} - \sigma_p}{\varepsilon}$$

where σ_{eff} is the stress of the polymer-MR fluid-filled lattice and σ_p is the stress of the pure polymer lattice. By measuring the hollow microlattice and MR fluid-filled microlattice at different magnetic field strengths, the relative stiffness of the MR fluid-filled microlattice was

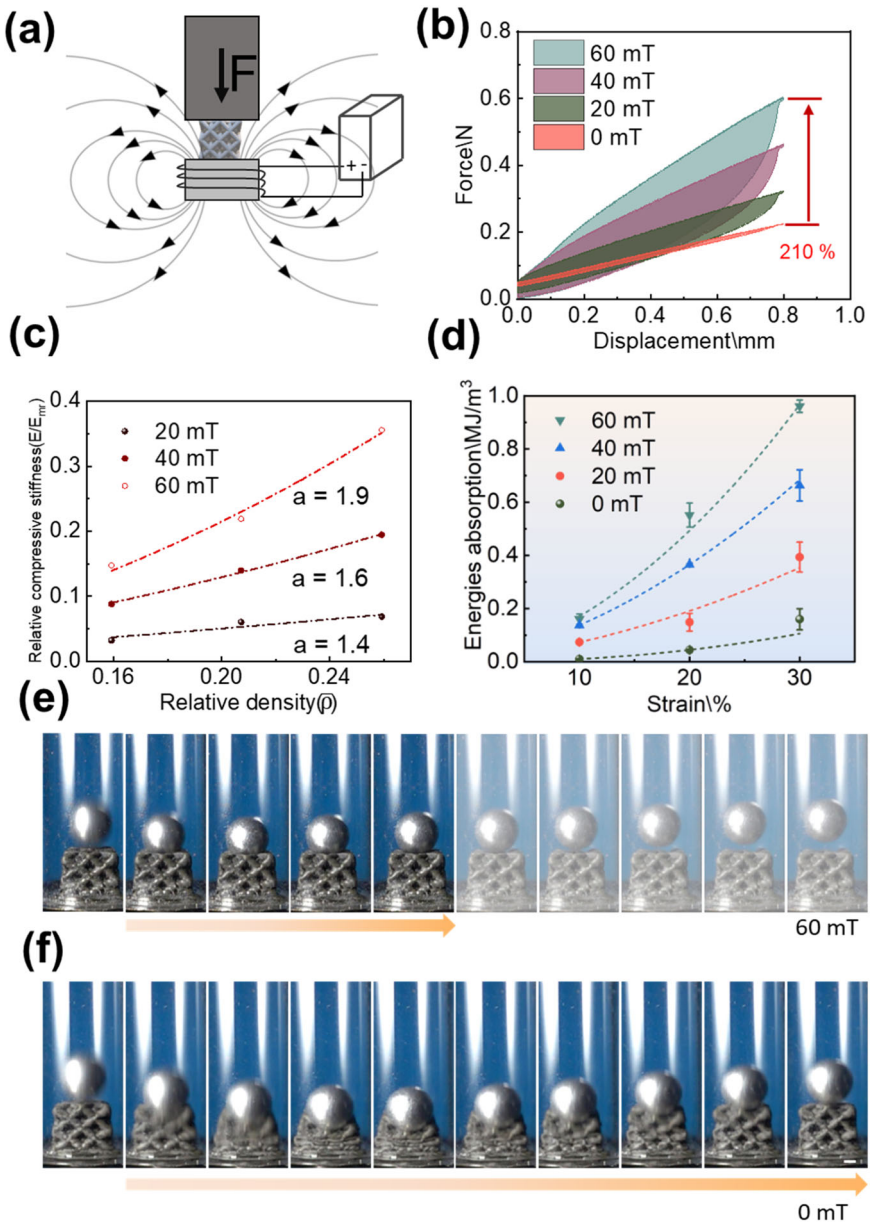

Fig. 3 Tunable mechanical properties of the MR fluid-filled microlattice by modulating the magnetic field. a Schematic of the experimental setup for mechanical testing of MR fluid-filled samples with magnetic field strength controlled by an adjustable DC power supply. **b** The stress–strain curves of octet microlattices under different magnetic field strengths. **c** The exponent *a* of the scaling law increases with increasing magnetic field strength. **d** Energy absorption as a function of deformation. The impact process of flexible magnetoactive microlattices. **e** When a magnetic field with a strength of 60 mT is applied, the magnetic lattice undergoes little deformation. **f** The lattice is severely compressed during the impact process once the magnetic field is removed. The interval of each frame is 20 ms.

obtained as a function of the MR fluid relative density (Fig. 3c). The exponent a ($E_{MR}/E_{mr} \propto (\overline{\rho}_{MR})^a$) increases from 1.4 to 1.9 as the magnetic field increases from 20 mT to 60 mT, where E_{mr} refers to the moduli of MR infillings, estimated by compression of the MR filled struts (the moduli at 20 mT, 40 mT, and 60 mT are 32 KPa, 61 KPa, and 92 KPa, respectively) and $\overline{\rho}_{MR}$ refers to the relative density of the MR filling of the lattice, as estimated by the volume fraction of MR filling. The exponent a is regarded as an indication of the deformation mode where a is 1 for ideal stretching-dominated behavior, and a is equal to 2 for bending-dominated behavior. The exponent a indicates that the deformation mode of the magnetoactive microlattice transforms from stretching-dominated to bending-dominated. The exponent a corresponds to the microstructure of the magnetic

field-triggered MR fluid. Considering the chain-like structure of the MR fluid, we hypothesize that the MR fillings have a hierarchical structure with lines of magnetic particles parallel to the magnetic field lines, as shown in Fig. S2. The applied strength of the magnetic field not only determines the intensity of induced magnetization but also increases the length of the chains of magnetic particles[39,40]. With the increase in lengths of particle chains, uniformly distributed particles are replaced by particle chains (Fig. S3). During the compression process, the longer magnetic lines bend more easily, changing the deformation mode and resulting in more dominance by bending in the deformation mode[26].

We further test their energy absorption under cyclic loading. Energy absorption is an important application of microlattice materials. Since no plateau strain[41] is observed in our magnetoactive microlattice, the energy absorption is evaluated in the linear stage and calculated by integrating the enclosed area of the loading–unloading curves (Fig. 3d). The energy absorption and strain have a relationship with $E \propto \varepsilon^2$. Compared with the energy absorption at 0 Tm, the magnetic field increases the energy absorption by 16.3, 12.4, and 6.0 times at strains of 10%, 20%, and 30% (Table S2).

Finally, we visually demonstrate the tunable stiffness and energy absorption of our MR fluid-filled microlattice metamaterial. A drop weight test is conducted with a 1.5 g aluminum ball that falls from height of 40 cm. The impact process is captured by a high-speed camera, and the results are shown in Fig. 3e, f (Video S4). In the presence of a relatively weak magnetic field with a strength of 60 mT, our MR fluid-filled microlattice does not undergo appreciable macroscopic deformation, and the impact process is finished in 80 ms. The impact process extends to 180 ms in the absence of a magnetic field. The MR fluid-filled microlattice undergoes severe deformation during the impact process.

Tuning the stress–strain responses on demand

Compared with previous magnetic materials that were controlled by powerful permanent magnets or Helmholtz coils requiring high voltage[18,42,43], this study demonstrates a magnetoactive metamaterial flexible enough to be actuated by a more easily controlled and safer electromagnet. Moreover, compared with the motion of a permanent magnet, an electromagnet can apply an accurate magnetic field in a shorter time. The field on and field off response times are measured to be 200 ms and 50 ms, respectively, in Fig. 4a, b where we adopt the criterion from a previous study[15]. The response time is a quarter of the previous result[15], which may be because the on-off of the electromagnet can build an accurate magnetic field in a shorter time than the movement of the permanent magnet.

The real-time response of our magnetoactive microlattice to a changing magnetic field leads to on-demand stress–strain curves or programmable mechanical properties. We design uniaxial compression with a strain rate of $3.3 \times 10^{-3}\ s^{-1}$ to prove the precise controllability of the stiffness based on a $2 \times 2 \times 2$ MR fluid-filled microlattice with polymer diameter of 1 mm and an MR fluid core diameter of 0.7 mm. During the compression process, we manually tune the magnetic field strength at displacements of approximately 0.5 mm, 1 mm, and 1.5 mm. Two groups of experiments are conducted. In the first group of experiments, the magnetic field strength is increased, as shown in Fig. 4a, while the magnetic field strength is decreased in the other experiment, as shown in Fig. 4b. To compare the mechanical response, the displacement–force curves under different field intensities are also plotted in Fig. 4a, b. As shown in Fig. 4a, the displacement–force curves track the displacement–force curves for 0 mT. When the magnetic field strength increases to 20 mT, an inflection point is observed, and the slope increases and finally follows the displacement–force curves for 20 mT. The same inflection points also occur when the magnetic field strength increases from 20 mT to 40 mT and from 40 mT to 60 mT. The forces finally accelerate to the corresponding force at 40 mT and 60 mT.

In the circumstance of a decreasing magnetic field, the force increases along with the displacement–force curves of 60 mT and dramatically drops when the magnetic field strength is decreased to 40 mT. The displacement–force curves coincide with the curves at 40 mT. A similar drop also occurs when tuning the magnetic field strength from 40 mT to 20 mT and from 20 mT to 0 mT. and then follows the curves under 20 mT to 0 mT, respectively. This experiment also indicates that remanence, which refers to the magnetization that remains in a magnetized substance after an external magnetic field is removed, is negligible in our MR fluid-filled microlattice.

Some potential applications of programmable mechanical metamaterials can be envisioned, such as artificial muscle, protection systems, and tactile perception. There are various design strategies for programmable mechanical metamaterials by architectural innovation. However, geometry-based programmable metamaterials rely on the deformation of materials, which means that the program is fixed once the metamaterials are fabricated[44]. In addition to difficult manipulation, the other current limitations are a narrow range of achievable moduli and relatively slow response times[44,45]. Our flexible magnetoactive metamaterial exploits these constraints and achieves the desired programmed force–displacement curves.

Summary

In summary, this study proposed a dual-phase liquid–solid magnetoactive microlattice metamaterial composed

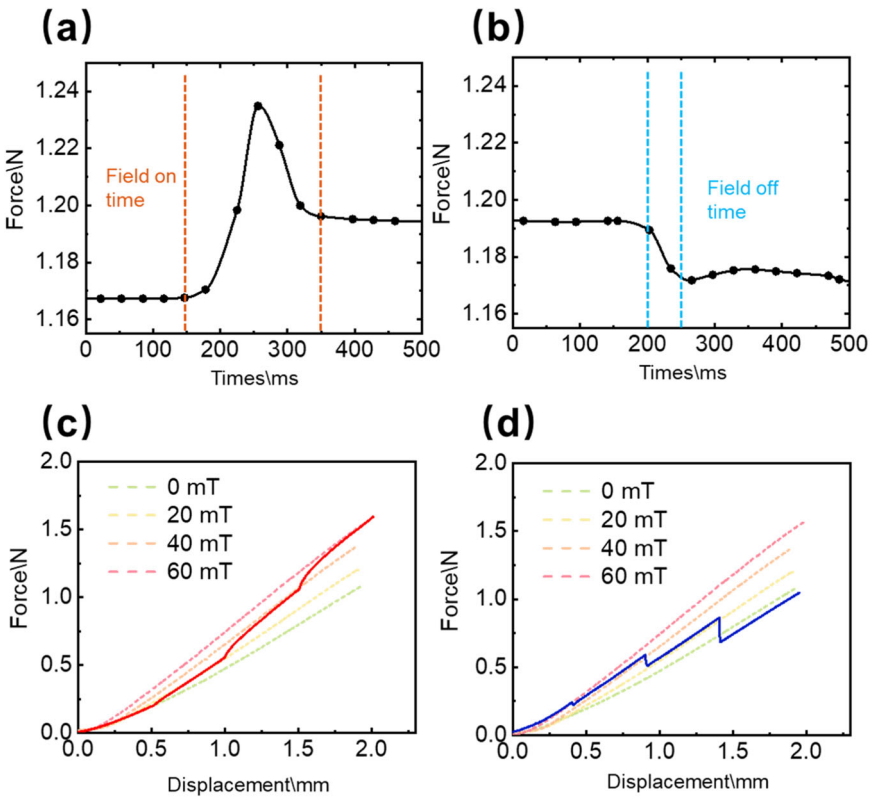

Fig. 4 Mechanical responses under compression with tunable stress–strain curves on demand. Mechanical response under a constant load **a** when the magnetic field increases from 0 mT to 60 mT and **b** when the magnetic field decreases from 60 mT to 0 mT. The corresponding plots of mechanical response for different programmed paths. The red and blue lines show the cases where all the magnetic field strengths increase **c** and decrease **d**, respectively. The dashed lines in **c**, **d** correspond to the microlattice metamaterial displacement–force curves at various magnetic field strengths.

of very flexible, 3D-printable polymer shells and magnetorheological fluids. These MR fluid-filled ultra-flexible magnetoactive microlattices were successfully fabricated by high-resolution stereolithography 3D printing technology and vacuum-assisted liquid filling. Our relatively large-scale microlattices demonstrated remarkable recoverability (~50%); moreover, our MR fluid-filled microlattices could be remarkably stiffened in the presence of a magnetic field with an ~200% increment in stiffness at 60 mT. Furthermore, the mechanical properties of this magnetoactive microlattice metamaterial could be modulated on demand, leading to programmable stress–strain behavior. These tunable properties characterized this mechanical metamaterial as a potential candidate for various emerging engineering applications.

Acknowledgements
We acknowledge financial support from the Science Technology and Innovation Commission of Shenzhen Municipality under type C grant SGDX20201103093003O1, the National Natural Science Foundation of China and Hong Kong Research Grant Council (RGC) joint research grant N_HKU159/22, and the City University of Hong Kong under grants 7020008 and 9667226. The authors also thank Dr. Zhifei Zhang of BMF Co., Ltd. and Mr. Zhuoqiang Zhang of Jilin University for their technical assistance.

Author details
[1]Department of Mechanical Engineering, City University of Hong Kong, Kowloon, Hong Kong SAR, China. [2]Nano-Manufacturing Laboratory (NML), City University of Hong Kong Shenzhen Research Institute, Shenzhen, China. [3]School of Environmental Science and Engineering, Southern University of Science and Technology, Shenzhen, China. [4]Department of Mechanical and Energy Engineering, Southern University of Science and Technology, Shenzhen, China. [5]Department of Mechanical Engineering, The University of Hong Kong, Pokfulam, Hong Kong SAR, China

Author contributions
Y.L. conceived and supervised the research. W.Z. designed and performed the experiments. W.Z. analyzed the data and wrote the manuscript. Y.L., Q.G., and W.Z. revised the paper. Y.J., J.C., and Y.P. assisted in part of the experiments and data analysis. J.Z., R.F., and F.M. helped analyze the mechanism. All authors discussed and approved the final manuscript.

Conflict of interest
The authors declare no competing interests.

Supplementary information The online version contains supplementary material available at https://doi.org/10.1038/s41427-023-00492-x.

Received: 26 October 2022 Revised: 6 July 2023 Accepted: 11 July 2023.
Published online: 25 August 2023

References

1. Yuan, C. et al. Thermomechanically triggered two-stage pattern switching of 2D lattices for adaptive structures. *Adv. Funct. Mater.* **28**, 1705727 (2018).
2. Roach, D. J., Kuang, X., Yuan, C., Chen, K. & Qi, H. J. Novel ink for ambient condition printing of liquid crystal elastomers for 4D printing. *Smart Mater. Struct.* **27**, 125011 (2018).
3. Boley, J. W. et al. Shape-shifting structured lattices via multimaterial 4D printing. *Proc. Natl Acad. Sci. USA* **116**, 20856–20862 (2019).
4. Zhang, K. et al. Reconfigurable network structure with tunable multiple deformation modes: mechanical designs, theoretical predictions, and experimental demonstrations. *Int. J. Solids Struct.* **260**, 112043 (2023).
5. Zhang, W. et al. Tailoring mechanical properties of PμSL 3D-printed structures via size effect. *Int. J. Extreme Manuf.* (2022).
6. Yu, H. et al. Metamaterials with a controllable thermal-mechanical stability: Mechanical designs, theoretical predictions and experimental demonstrations. *Compos. Sci. Technol.* **207**, 108694 (2021).
7. Chen, T., Pauly, M. & Reis, P. M. A reprogrammable mechanical metamaterial with stable memory. *Nature* **589**, 386–390 (2021).
8. Kim, Y., Yuk, H., Zhao, R., Chester, S. A. & Zhao, X. Printing ferromagnetic domains for untethered fast-transforming soft materials. *Nature* **558**, 274–279 (2018).
9. Zhang, H., Guo, X., Wu, J., Fang, D. & Zhang, Y. Soft mechanical metamaterials with unusual swelling behavior and tunable stress-strain curves. *Sci. Adv.* **4**, eaar8535 (2018).
10. Gladman, A. S., Matsumoto, E. A., Nuzzo, R. G., Mahadevan, L. & Lewis, J. A. Biomimetic 4D printing. *Nat. Mater.* **15**, 413–418 (2016).
11. Huang, T.-Y. et al. Four-dimensional micro-building blocks. *Sci. Adv.* **6**, eaav8219 (2020).
12. Kuang, X., Roach, D. J., Hamel, C. M., Yu, K. & Qi, H. J. Materials, design, and fabrication of shape programmable polymers. *Multifunctional Mater.* **3**, 032002 (2020).
13. Lu, H. et al. A bioinspired multilegged soft millirobot that functions in both dry and wet conditions. *Nat. Commun.* **9**, 3944 (2018).
14. Ge, Q. et al. 3D printing of highly stretchable hydrogel with diverse UV curable polymers. *Sci. Adv.* **7**, eaba4261 (2021).
15. Xia, X., Spadaccini, C. M., & Greer, J. R. Responsive materials architected in space and time. *Nat. Rev. Mater.* 1–19 (2022).
16. Xia, X. et al. Electrochemically reconfigurable architected materials. *Nature* **573**, 205–213 (2019).
17. Lau, G.-K., Heng, K.-R., Ahmed, A. S. & Shrestha, M. Dielectric elastomer fingers for versatile grasping and nimble pinching. *Appl. Phys. Lett.* **110**, 182906 (2017).
18. Kim, Y., Parada, G. A., Liu, S. & Zhao, X. Ferromagnetic soft continuum robots. *Sci Robot.* **4**, eaax7329 (2019).
19. Lu, H., Hong, Y., Yang, Y., Yang, Z. & Shen, Y. Battery-less soft millirobot that can move, sense, and communicate remotely by coupling the magnetic and piezoelectric effects coupling the magnetic and piezoelectric effects. *Adv. Sci.* **7**, 2000069 (2020).
20. Wang, Y., Li, L., Hofmann, D., Andrade, J. E. & Daraio, C. Structured fabrics with tunable mechanical properties. *Nature* **596**, 238–243 (2021).
21. Wang, Y. et al. Architected lattices with adaptive energy absorption. *Extreme Mech Lett.* **33**, 100557 (2019).
22. Deshmukh, S. S. & McKinley, G. H. Adaptive energy-absorbing materials using field-responsive fluid-impregnated cellular solids. *Smart Mater. Struct.* **16**, 106 (2006).
23. Han, W., Gao, W. & Wang, X. A novel magneto-mechanical metamaterial cell structure with large, reversible and rapid two-way shape alteration. *Smart Mater Struct.* **30**, 035018 (2021).
24. Yu, K., Fang, N. X., Huang, G. & Wang, Q. Magnetoactive acoustic metamaterials. *Adv. Mater.* **30**, e1706348 (2018).
25. Jackson, J. A. et al. Field responsive mechanical metamaterials. *Sci. Adv.* **4**, eaau6419 (2018).
26. Bauer, J. et al. Nanolattices: an emerging class of mechanical metamaterials. *Adv Mater.* **29**, 1701850 (2017).
27. Zhang, X., Wang, Y., Ding, B. & Li, X. Design, fabrication, and mechanics of 3D micro-/nanolattices. *Small* **16**, e1902842 (2020).
28. Surjadi, J. U. et al. Mechanical metamaterials and their engineering applications. *Adv. Eng. Mater.* **21**, 1800864 (2019).
29. Ge, Q. et al. Projection micro stereolithography based 3D printing and its applications. *Int. J. Extreme Manuf.* **2**, 022004 (2020).
30. Zhang, W., Chen, J., Li, X. & Lu, Y. Liquid metal-polymer microlattice metamaterials with high fracture toughness and damage recoverability. *Small* **16**, e2004190 (2020).
31. Lin, Y. et al. Vacuum filling of complex microchannels with liquid metal. *Lab Chip.* **17**, 3043–3050 (2017).
32. Messner, M. C. Optimal lattice-structured materials. *J. Mech. Phys. Solids* **96**, 162–183 (2016).
33. Zhang, X. et al. Three-dimensional high-entropy alloy-polymer composite nanolattices that overcome the strength-recoverability trade-off. *Nano Lett.* **18**, 4247–4256 (2018).
34. Schwaiger, R., Meza, L. & Li, X. The extreme mechanics of micro-and nanoarchitected materials. *MRS Bull.* **44**, 758–765 (2019).
35. Valdevit, L., Godfrey, S. W., Schaedler, T. A., Jacobsen, A. J. & Carter, W. B. Compressive strength of hollow microlattices: experimental characterization, modeling, and optimal design. *J. Mater. Res.* **28**, 2461–2473 (2013).
36. Wang, Y., Zhang, X., Li, Z., Gao, H. & Li, X. Achieving the theoretical limit of strength in shell-based carbon nanolattices. *Proc. Natl Acad. Sci. USA* **119**, e2119536119 (2022).
37. Hongyun, W., Cheng, B., Junwu, K., Chunfu, G. & Wang, X. The mechanical property of magnetorheological fluid under compression, elongation, and shearing. *J. Intel. Mat. Syst. Str.* **22**, 811–816 (2011).
38. Zheng, X. et al. Ultralight, ultrastiff mechanical metamaterials. *Science* **344**, 1373–1377 (2014).
39. Wang, N. et al. Microscopic characteristics of magnetorheological fluids subjected to magnetic fields. *J. Magnetism Magnet. Mater.* **501**, 166443 (2020).
40. Ji, D., Luo, Y., Ren, H., Wei, D. & Shao, J. Numerical simulation and experimental analysis of microstructure of magnetorheological fluid. *J. Nanomater.* **2019**, 1–17 (2019).
41. Meng, M. et al. Design of negative curvature fiber carrying multiorbital angular momentum modes for terahertz wave transmission. *Results Phys.* **29**, 104766 (2021).
42. Ze, Q. et al. Magnetic shape memory polymers with integrated multifunctional shape manipulation. *Adv. Mater.* **32**, e1906657 (2020).
43. Yang, X. et al. An agglutinate magnetic spray transforms inanimate objects into millirobots for biomedical applications. *Sci Robot.* **5**, eabc8191 (2020).
44. Florijn, B., Coulais, C. & van Hecke, M. Programmable mechanical metamaterials: the role of geometry. *Soft Matter* **12**, 8736–8743 (2016).
45. Bauer, J., Guell Izard, A., Zhang, Y., Baldacchini, T. & Valdevit, L. Programmable mechanical properties of two-photon polymerized materials: from nanowires to bulk. *Adv. Mater. Technol.* **4**, 1900146 (2019).